Extracellular carotenoid production and fatty acids profile of *Parachlorella kessleri* under increased CO_2 concentrations

Priscila da Costa Carvalho de Jesus [a], Maria Anita Mendes [a], Elen Aquino Perpétuo [b,c],
Thiago Olitta Basso [a], Claudio Augusto Oller do Nascimento [a,*]

[a] *Department of Chemical Engineering, Escola Politécnica, Universidade de São Paulo, São Paulo, Brazil*
[b] *Centro de Estudos e Pesquisa em Meio Ambiente (CEPEMA), Universidade de São Paulo, Cubatão, Brazil*
[c] *Institute of Marine Sciences, Universidade Federal de São Paulo (UNIFESP), Santos, Brazil*

A B S T R A C T

Large-scale cultivations of photoautotrophic microorganisms represent a very promising and potentially cost-effective alternative for climate change mitigation, when associated to the co-production of high value bio-products, such as fatty acids and carotenoids, considering the growing demand for natural products. During microalgae cultivation, CO_2 enrichment is a requirement to reach high productivities, although high CO_2 levels are normally stressful to microalgae. On the other hand, cellular stress is a well reported strategy to induce carotenoid and fatty acids production. This work evaluated extracellular carotenoid production from the mangrove-isolated microalga *Parachlorella kessleri* cultivated under 5, 15 and 30% CO_2 in stirred tank photo-bioreactors. In the 10th day of cultivation, CO_2 supply was interrupted until the end of the cultivation (14th day), causing a stressful and imperative condition for microalgae cells to release the red pigment. Growth kinetics, physiological parameters and bioproducts production were evaluated. Growth kinetics were similar under all tested conditions and differences were not statistically significant, with the highest values of μ_{max}, biomass concentration, lipid content and CO_2 fixation rate of 0.77 d^{-1}, 1.24 g L^{-1}, 241 mg g^{-1} (dw) and 165 mg L^{-1} d^{-1}, respectively. In contrast, total carotenoid concentrations varied significantly ($p < 0.01$), with the highest concentration of 0.030 μg mL^{-1} under 5% CO_2. The produced red pigment presented antioxidant activity and characteristics of carotenoids confirmed by UV–vis and tandem mass spectrometry (MS/MS). The fatty acid profiles in the biomass varied in response to CO_2 levels in the cultivations. In general, higher CO_2 concentrations (15 and 30%) favored the production of saturated and mono-unsaturated fatty acids, suitable as biodiesel feedstock, while drastically decreased the production of the polyunsaturated.

1. Introduction

Carbon dioxide (CO_2) fixation using fast-growing photoautotrophic microorganisms, especially microalgae, in their natural habitats or in artificial cultivation systems, provides a very promising alternative for climate change mitigation. Besides, it is potentially cost-effective when CO_2 conversion is associated to the co-production of high value bio-products (Borowitzka, 2013). There are various sources of CO_2 for autotrophic microalgae cultivation in addition to atmospheric air (which contains approximately 380 ppm, 0.04%). For instance, CO_2 can be sourced from flue gas of industrial plants (10–20% CO_2) (Yadav et al., 2015; Wilson et al., 2016), or provided by natural gas (around 8%) (Balcombe et al., 2015) and biogas (30–40%) (van der Ha et al., 2012).

However, microalgae respond differently to CO_2 levels, as well as to oxygen concentrations, light intensities, nutrients, pH and temperature (Salih, 2011). Therefore, it is important to select high CO_2-tolerant microalgae for cultivations using gaseous sources with high CO_2 levels.

Parachlorella kessleri has been reported to grow under CO_2 levels up to 18%, with the highest growth rate at 6% CO_2 (Klinthong et al., 2015; de Morais and Costa, 2007). When cultivated in photobioreactor, *P. kessleri* presented high growth rates, tolerance to high temperatures, resistance to shear stress, little adhesion to the bioreactor surfaces and low tendency to form aggregates (Li et al., 2013). Although *P. kessleri* is regarded as a starch producer for energy storage, hyper-production of lipids was achieved (60% dw) by optimal growth conditions under 2% CO_2, followed by 5- to 10-fold dilution of the culture medium after the

exponential growth phase (Li et al., 2013).

Microalgae have been used to convert CO_2 into a wide variety of industrially-relevant bioproducts. Microalgal lipids are a rich source of fatty acids (FA), such as linoleic acid, arachidonic acid, eicosapentaenoic acid (EPA) and docosahexanoic acid (DHA), for cosmetic, pharmaceutical and nutraceutical applications (Borowitzka, 2013). They have also been widely reported as suitable feedstock for biodiesel (Chisti, 2007), although its production is only economically viable when associated to co-production of higher value products from microalgal biomass, such as carotenoids, vitamins, phycobilins, sterols, polyhydroxyalkanoates and polysaccharides (Gracioso et al., 2020; Borowitzka, 2013).

Among the reported carotenoids produced by microalgae, astaxanthin is the compound with the highest value that has achieved commercial success. For instance, the worldwide market for astaxanthin (both from synthetic and natural sources) in 2010 was around US\$ 230 million, with average market price of US\$ 2500 kg^{-1}, which decreased to almost US\$ 1900 kg^{-1} in 2014 (Cezare-Gomes et al., 2019). Consumers demand for natural products has made synthetic pigments much less desirable, providing an opportunity for the production of natural pigments. Other potential carotenoids are lutein and zeaxanthin, already approved as food additives for preventing macular diseases (Krinsky et al., 2003). Currently, the main sources of lutein for commercial production are marigold flowers, and there is no commercial production of lutein from microalgae (Cezare-Gomes et al., 2019). *P. kessleri* was reported to produce astaxanthin and lutein at production rates of 0.07 mg L^{-1}d^{-1} and 0.04 mg L^{-1}d^{-1}, respectively (Minhas et al., 2016).

The production of carotenoids in microalgae occurs, in some cases, when they are subjected to stress. During microalgae cultivation, CO_2 enrichment is a requirement to reach high productivity. On the other hand, high CO_2 levels are normally stressful to microalgae, especially for the photosynthetic apparatus, which can induce carotenoid production (Chekanov et al., 2017). Likewise, high CO_2 levels can stimulate the production of FA, with applications for biofuels or as nutraceuticals and pharmaceuticals (Sun et al., 2016).

The aim of the present report was to evaluate extracellular carotenoid production by *P. kessleri* in cultivations in stirred tank photobioreactor under increased CO_2 concentrations, for future applications using gaseous sources with high CO_2 levels. In addition, the FA profiles were investigated to identify potential industrial applications of the produced biomass.

2. Materials and methods

2.1. Parachlorella kessleri cultivation

Fast-growing *P. kessleri* was isolated from water and sediment samples of mangroves near Cubatão and Guarujá, municipalities in the metropolitan area of Baixada Santista in the coast of the state of São Paulo (Brazil). The strain was first adapted to elevated CO_2 concentration by cultivations in 1,150 mL gas sealed flasks filled with 200 mL of WC medium (Andersen et al., 2004) at fixed temperature (28 °C), rotation (120 rpm) and light intensity of approximately 25 µmol s^{-1} m^{-2} provided by LED (3,500 K) with 14 h/10 h light/dark photoperiod. The atmosphere on the headspace of the flask was filled with air enriched with 30% CO_2 (v/v), at a flow rate of 0.5 L min^{-1} for 3 min using a mass flow controller (MKS Instruments), and was renovated on a daily basis. Replications occurred every 10 days until 4 repetitions, obtaining a high CO_2-tolerant microalga. *P. kessleri* stocks were maintained at 19 °C and approximately 25 µmol photons m^{-2} s^{-1} of light intensity.

2.2. Photobioreactor apparatus and operational conditions

Two identical stirred tank bioreactors (A and B) of 3.6 L (Infors HT) were used for simultaneous replicates. They worked in batch mode and were initially filled with 1.5 L of WC medium. Temperature was controlled at 28 °C, through water jacket, and agitation of 120 rpm was promoted by a pitched paddle impeller. Luminosity was promoted by an especially designed LED panel around the vessel with average intensity inside the vessel of 45 µmol s^{-1} m^{-2} (14 h/10 h light/dark). The gas inlet was positioned to fill the headspace of the reactor, and was composed of air enriched with CO_2 in concentrations of 5, 15 and 30% (v/v). This operational configuration was based on the hypothesis that the consumption of CO_2 by the microalgae is very low when compared to available CO_2 (da Silveira, 2015) (when working with high CO_2 levels), thus CO_2 daily supply would be sufficient to keep its concentration inside the reactor nearly constant. A mass flow controller (MKS Instruments) was used to mix the gases at specific flow rates to give the desired final CO_2 concentration and feed the reactor at 0.5 L min^{-1} for 30 min during the light period. The gas inlet and outlet were then closed until the following atmosphere renovation after 24 h. Sensors of pH and dissolved oxygen allowed the monitoring of both parameters, respectively.

2.3. Kinetic assays of P. kessleri under different CO_2 concentrations

Pre-inoculum was prepared by cultivating *P. kessleri* from the stocks in 500 mL shake flask with cotton plug containing WC medium to give a total volume of 300 mL and initial optical density at 750 nm (OD$_{750nm}$) of 0.2. Cultivation was performed at 28 °C, average light intensity of 25 µmol photons m^{-2} s^{-1}, 14 h/10 h (light/dark) photoperiod, in rotational incubator (Infors HT) at 120 rpm. After the adaptation period of 96 h, microalgae in exponential growth phase were used as inocula. The photobioreactors were inoculated with *P. kessleri* adjusted to initial OD$_{750nm}$ of 0.1. The assays were performed under CO_2 concentrations of 5, 15 and 30% (v/v) in air. On the 10th day, atmosphere renovation was interrupted until the end of the cultivation. This is believed to cause a stress on microalgal cells and is an imperative condition to make them release the reddish pigment. Samples of 10–15 mL were withdrawn from the reactors on a daily basis, using the aseptic sampling system Super Safe Sampler (Infors HT) and a needle-free syringe, to evaluate microalgae growth and chlorophyll-a (Chl-a) profiles. Dissolved oxygen and pH were continuously monitored during the cultivation period. On the 14th day of cultivation, the batch was stopped; the biomass was harvested and centrifuged at 3,000g for 5 min. The supernatant of each cultivation was separated and stored in amber flasks (to protect from light) at 4 °C, for further purification and characterization, and the biomass was frozen at −80 °C for 12 h, lyophilized (Freezone 4.5, LabConco), and stored at 4 °C for lipid and elemental (C,N,H) analyses (Perkin Elmer 2400 series ii).

2.4. Lipid extraction

For lipid extraction, the classic Bligh & Dyer (Bligh and Dyer, 1959) method with modifications from Masood et al. (2005) was used. The lyophilized biomass of the 14th day of all cultivations was weighed and 100 mg were diluted with 2.5 mL of chloroform/methanol (1/2 v/v) in glass tubes. The tubes were placed in ultrasonic bath at room temperature for 1 h, when 1 mL of chloroform and 1.8 mL of Milli-q water were added, followed by vigorous agitation. The samples were centrifuged at 1,000g for 5 min to separate the phases and the organic phase was transferred to a fresh and pre-weighed tube. Following extractions with 1 mL of chloroform were performed until the biomass was colorless, after each transferring the organic phase to the tube containing the organic phases of previous extractions. Solvent was evaporated using a vacuum concentrator (CentriVap, LabConco), and the tube was then weighed to determine total lipid content and stored at −20 °C for FA analysis.

2.5. Fatty acid analysis

The lipid extracts reacted with 3 mL of methanol containing 5% (v/v) of sulfuric acid for 3 h at 70 °C to produce the respective fatty acid

methyl esters (FAME). After the transesterification reaction, 3 mL of *n*-hexane and 3 mL of Milli-q water were added (Breuer et al., 2013). The tubes were agitated and the hexane phase was collected. A volume of 1 µL of each sample was injected in the gas chromatograph coupled to mass spectrometer (GCMS-QP2010 Plus, Shimadzu) with electrons ionization (70 eV) and quadrupole analyzer. The analyses were conducted using a DB-5 capillary column (Agilent) 30 m x 0,25 mm x 0,25 µm and the following temperature program: temperature of injection of 280 °C, initial and final temperatures of the column of 40 °C and 300 °C, respectively, with heat rate of 3 °C min^{-1}. A FAME standard (Sigma) was also injected to identify the FA in the samples based on different retention times. The ion source and interface temperatures were both 300 °C. The mass spectra were acquired using the scan mode with *m/z* ranging from 50 to 700. FAME were identified using the NIST Standard Reference Database.

2.6. Analytical methods and calculations

Microalgae growth was evaluated by OD$_{750nm}$ measures, using a UV–vis spectrophotometer (UV-2600, Shimadzu), every 24 h during the 14-day cultivation. Maximum specific growth rates (µ$_{max}$) were estimated by the slope of the linear plot between the natural logarithm of OD$_{750nm}$ readings and time, during the exponential phase of growth.

Cell dry weight (CDW) concentrations were determined in the harvested biomass and performed in duplicate for each cultivation. First, 0.45 µm nitrocellulose membrane filters (Millipore) were dried for 12 h at 70 °C, cooled down in a vacuum desiccator, and weighed until constant weight. An aliquot of 10 mL of the algal suspension was vacuum filtered and the membrane with wet biomass was dried in a microwave oven for 10 min at low power. The dry biomass and membrane was then weighed to constant weight and membrane's weight was subtracted. Cellular concentration (X) was calculated by dividing CDW by the volume (10 mL) (Zhu and Lee, 1997).

Carbon dioxide fixation rates (PCO$_2$) were calculated using Eq. 1 (Kassim and Meng, 2017), where MCO$_2$ and MC are the molecular weight of CO$_2$ (44 g mol^{-1}) and C (12 g.mol^{-1}), respectively, C$_c$ is average carbon content in the dry biomass according to elemental analysis and P (g.L^{-1}.d^{-1}) is microalgal biomass productivity (Eq. 2).

$$PCO_2 = C_C P x \left(\frac{MCO_2}{MC}\right)$$ (1)

$$P = \frac{X_{final} - X_{initial}}{t_{final} - t_{initial}}$$ (2)

Chlorophyll-a was extracted from appropriate volumes of biomass samples with methanol for 30 min, in the dark, at 45 °C to give an absorbance at 680 nm between 0.1 and 0.7 (Pruvost et al., 2011). Absorbance was measured at 652, 665 and 750 nm and Chl-a concentrations were calculated by Eq. 3 (Ritchie, 2006).

$$[Chl-a]\left[\frac{\mu g}{mL}\right] = 8.0962(A_{652} - A_{750}) + 16.5169(A_{665} - A_{750})$$ (3)

Total carotenoids were spectrophotometrically quantified in the supernatant by absorbance measures at 450 nm and using Eq. 4, where $A_{1cm}^{1\%}$ is the molar extinction coefficient of 2,500 (Britton, 1985) and V is the volume of sample that gives the absorbance A$_{450}$ between 0.1 and 0.5 (50 mL).

$$Carotenoid\ content\ (\mu g\ mL^{-1}) = \frac{A_{450} \cdot 10^4}{A_{1cm}^{1\%} \cdot V}$$ (4)

Statistical analysis on the calculated parameters was conducted using the *Prism 6.0* software by application of the *One-way ANOVA* analysis to determine the statistical significance of data differences (p < 0.05), with *Tukey* test as the post-test applied.

2.7. Carotenoid characterization

2.7.1. Pre-purification

The pigments were pre-separated by passing 50 mL of each supernatant of the end of the cultivation to a packed C18 silica column for solid phase extraction (Sep-Pak Vac Cartridge 20cc, Waters), with particle size of 55–105 µm, similar in behavior to reversed-phase HPLC columns, under vacuum pressure. The pigments were retained in the column and were then eluted with 5 mL of methanol (HPLC grade, Merck) (Fig.1).

2.7.2. Antioxidant activity

Trolox equivalent antioxidant capacity (TEAC) was used to evaluate the antioxidant capacity of the extracellular pigments by comparison to Trolox (6-hydroxy-2,5,7,8-tetramethylchroman-2-carboxylic acid) antioxidant capacity. The quantitative assessment of antioxidant activity against the radical ABTS$^{\bullet+}$ (2,2'-Azino-bis(3-ethylbenzothiazoline-6-sulfonic acid) was performed using spectrophotometric measures (UV-2600, Shimadzu) of the consumption of the radical in the presence of antioxidant substances (Re et al., 1999).

2.7.3. High performance liquid chromatography (HPLC) separation

A semi-preparative HPLC (Shimadzu) equipped with PDA detector and automatic fraction collector was used to identify and separate the carotenoids. The methanolic extracts, previously filtered at 0.22 µm, were injected in a C18 reverse phase column (Zorbax, 9.4 mm x 250 mm x 5 µm). As a mobile phase, the following program with acetonitrile (Merck, HPLC grade) and Milli-q water containing 0.1% (v/v) of acetic acid was used: 0–2 min, isocratic 5% acetonitrile; 2–32 min, linear gradient of acetonitrile 5–80%; 32–35 min, isocratic acetonitrile 80%; 35–40 min, isocratic acetonitrile 5%. The flow rate of the mobile phase was 3 mL min^{-1}, the column temperature 40 °C and the injection volume was 1000 µL. The detection was made at 320 nm and absorption spectrum in the UV–vis range.

2.7.4. Liquid chromatography coupled to mass spectrometry (LC–MS/MS IT-TOF) analysis of the carotenoid fractions

The two carotenoid fractions separated in the semi-preparative HPLC were N$_2$ dried, dissolved in 200 µL of methanol (Merck, HPLC grade) and passed through a 0.22 µm filter (Millipore) before injection. The carotenoids were qualitatively verified using a Shimadzu LC-IT-TOF-MS. This hybrid instrument is an integration of ultra-high-performance liquid chromatography (UHPLC) with IT-TOF-MS, a high-resolution mass spectrometer. The UHPLC system (Shimadzu) consisted of a gradient pump (LC-20AD), an autosampler (SIL-20AC), a degasser (DGU-20A3), a
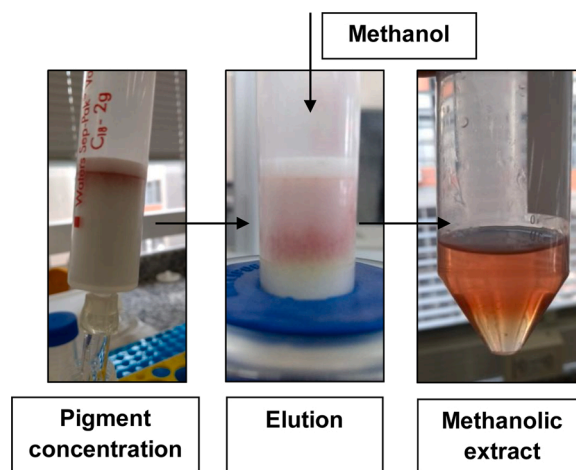

Fig. 1. Pigments pre-purification steps in Sep-Pak C18 column and elution with methanol.

communication bus module (CBM-20A), and a column oven (CTO-20AC). The analytes were separated using a Shim-pack XR-ODS column (Shimadzu, 2.0 mm x 30 mm) at oven temperature of 40 °C and flow rate of 0.2 mL min^{-1}. The injection volume was 5 μL. The mobile phase consisted of acetonitrile (Merck, HPLC grade) and Milli-q water with 0.1% (v/v) of acetic acid (0–2 min, isocratic with 5% acetonitrile; 2–15 min, linear gradient of 5–80% acetonitrile; 15–17 min, isocratic with 80% acetonitrile; 17-18 min, isocratic with 5% acetonitrile). The detection was performed by PDA detector at 320 nm. The hybrid IT-TOF-MS high-resolution spectrometer had an electrospray ionization (ESI) source that operated in positive mode. The MS conditions were as follows: nebulizer gas (N$_2$) flow rate, 1.5 L min^{-1}; drying gas (N$_2$) pressure, 100 kPa; curved desolvation line temperature, 200 °C; block heater temperature, 200 °C; detector voltage, 1.63 kV; electrospray voltage, 4.5 kV; mass range, *m/z* 50–1,000 (MS^1 and MS^2); TOF pressure, 1.3×10^{-4} Pa; IT pressure, 1.8×10^{-4} Pa; ion accumulation time, 10 msec. The LC–MS/MS data were collected and processed by LabSolutions software (Shimadzu).

3. Results

3.1. Growth kinetics of P. kessleri under different CO$_2$ concentrations

In general, *P. kessleri* displayed different growth and product formation kinetics under different CO$_2$ concentrations. Growth profiles under 5 and 15% CO$_2$ were similar, while under 30% CO$_2$ growth was slower than in the other conditions after the end of the exponential phase (Fig. 2). The exponential growth phases, determined from the slope of the linear plot between the natural logarithm of OD$_{750nm}$ readings and time, occurred from day 0 to day 4 under 5% CO$_2$, from day 0 to day 3 or 4 (depending on the assay) under 15% CO$_2$ and from day 1 to day 3 or 4 (depending on the assay) under 30% CO$_2$. The calculated maximum specific growth rates were 0.74 ± 0.09, 0.74 ± 0.08 and 0.77 ± 0.11 d^{-1} under 5, 15 and 30% CO$_2$, respectively, and the differences were not statistically significant (p > 0.05) (Fig. 3a). CDW concentrations on the 14th day of cultivation (Fig. 3b) were 1.09 ± 0.12, 1.24 ± 0.15 e 1.09 ± 0.25 g L^{-1}, and CO$_2$ fixation rates (calculated using Eq. 1, Fig. 3c) were 158 ± 7, 165 ± 5 and 141 ± 3 mg L^{-1}d^{-1}, under 5, 15 and 30% CO$_2$, respectively, obtained from carbon content in the biomass of 52.0, 47.5 and 48.5% for 5, 15 and 30% CO$_2$, respectively.

Interestingly, specific growth rates in this work were 2.5–3 fold higher than the ones obtained by de Morais and Costa (2007) with *Chlorella kessleri*: 0.257, 0.267, 0.267 and 0.199 d^{-1} under 0.04, 6, 12 and 18% CO$_2$, respectively. The differences compared to our work that

Fig. 3. Physiological parameters of *P. kessleri* cultivations in photobioreactor under 5, 15 and 30% CO$_2$: maximum specific growth rate (μ$_{max}$) (a), biomass concentration (dw) on the 14th day of cultivation (b), and CO$_2$ fixation rate (c). The error bars are the standard deviation of the mean of 4 repetitions.

probably can explain the higher growth rates are several: the type of bioreactor (we used stirred tank with constant agitation at 120 rpm), the light source (we used LED, which provides light within a narrower range of wavelengths than fluorescent lamps (Yan et al., 2016)), the volume of headspace in the reactor (we used almost 2 L instead of 200 mL; this headspace is necessary to improve gas-liquid mass transfer (Fung, 2002)). In addition, in our work the *P. kessleri* strain was first adapted to 30% CO$_2$, and in de Morais and Costa (2007) the strain was adapted and maintained in 1% CO$_2$.

Likewise, the reported maximum biomass concentrations by de Morais and Costa (2007) were lower than our results, except for the condition of atmospheric CO$_2$ (0.04%). The following values were obtained: 1.45, 0.98, 0.80 and 0.88 under 0.04, 6, 12 and 18% CO$_2$, respectively. In the same report, CO$_2$ fixation rate under 18% CO$_2$ was 163 mg L^{-1}d^{-1}, similar to the one obtained in this work, under 15% CO$_2$. Higher values of CO$_2$ fixation rate from 251 to 1,500 mg L^{-1}d^{-1} have been reported for other microalgae, such as *Dunaliella tertiolecta*, *Chlorella vulgaris*, *Spirulina platensis*, *Botryococcus braunii* and *Synechocystis*
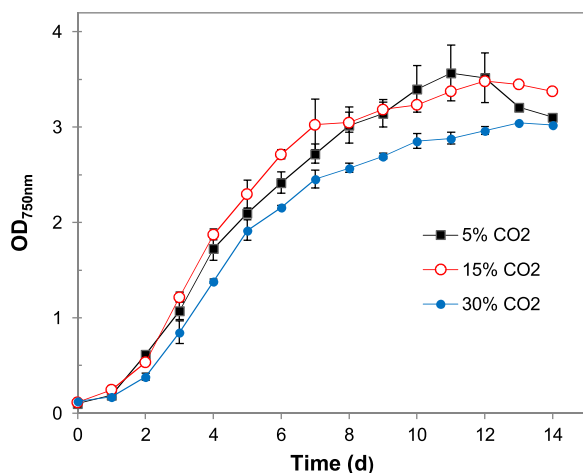

Fig. 2. Growth kinetics of the mangrove-isolated *P. kessleri* in photobioreactor under CO$_2$ concentrations of 5, 15 and 30%. The error bars are the standard deviation of the mean of 4 repetitions.
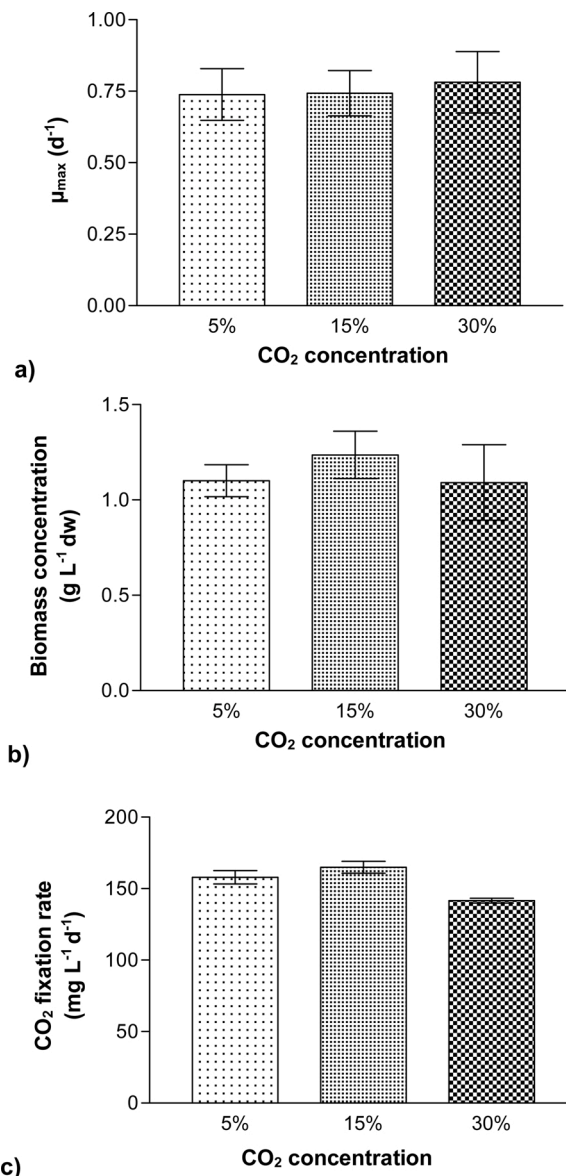
aquatilis (Singh and Singh, 2014).

The pH values in the culture medium varied considerably among the cultivation conditions (Fig. 4). Initial pH values right after inoculation were approximately 5.8, 5.5 and 5.0 for 5, 15 and 30% CO_2, respectively. Right after aeration supplied with CO_2 in the reactor, the balance $HCO_3^- + H^+ \leftrightarrow CO_2 + H_2O$ in the liquid is shifted to the formation of H^+, decreasing pH; the more CO_2, the lower the pH. The oscillations during one-day period are regarded to the light/dark photoperiods, while sudden pH drops, pointed with arrows in Fig. 4, correspond to the moment of atmosphere renovation. During phototrophic growth, in the light period, microalgae consume CO_2 and produce O_2. Thus, with no pH control or buffer solution, the pH tends to increase according to growth, as more microalgae consume more CO_2, and the balance of the $HCO_3^- + H^+ \leftrightarrow CO_2 + H_2O$ reaction is then shifted to the formation of CO_2 and H_2O, decreasing the concentration of H^+ and consequently increasing the pH. On the other hand, in the dark period, microalgae consume O_2 and produce CO_2 during respiration, decreasing pH.

Under 5% CO_2, pH increased from 5.7 on the first day to 10.5 on the 5th day, decreased until the 10th day, and increased again until the end of the cultivation, because of interruption on CO_2 supply in the reactor. On the cultivations under 15% CO_2, the highest pH values during exponential phase were around 6.5. However, from day 12–14, pH abruptly increased and reached 10.5, when probably most of the CO_2 in the medium was consumed. Contrasting to pH profiles under 5 and 15% CO_2, under 30% CO_2 pH remained within a narrower range, varying around 5–6 during the whole cultivation period. Under this CO_2 condition, closing the gas inlet, and consequently interrupting the atmosphere renovation inside the photobioreactor, did not seem to interfere on its CO_2 concentration and, therefore, on the pH of the culture medium.

Chlorophyll-a profiles (Fig. 5) exhibited the highest values of Chl-a concentrations on days 4 and 5 of cultivation, decreasing until the end of the cultivation. This may be explained by a nitrogen limitation in the medium followed by degradation in nitrogen internal sources, such as chlorophylls (Pruvost et al., 2011). Similar Chl-a profiles were described by Li et al. (2015) in cultivations using *Chlorella* sp. previously adapted to 10 and 20% of CO_2. In this work, we did not directly measure the consumption of nitrogen; however, nitrogen percentages in the biomass were indeed measured by elemental analysis on days 3 and 14. The results showed an overall decrease from 5.26% (day 3) to 1.18% (day 14), in average.

3.2. Lipid content and FA composition of P. kessleri under different CO_2 concentrations

The lipid content and FA composition of *P. kessleri* cultivated under varying CO_2 concentrations (5, 15 and 30%) were evaluated during non-limited nitrogen requirement. Total lipid contents were 241 ± 11, 208 ± 5 e 183 ± 14 mg g^{-1} of biomass (dw) under 5, 15 and 30% CO_2, respectively. (Minhas et al., 2016) reported 21.42% (dw) of lipid content
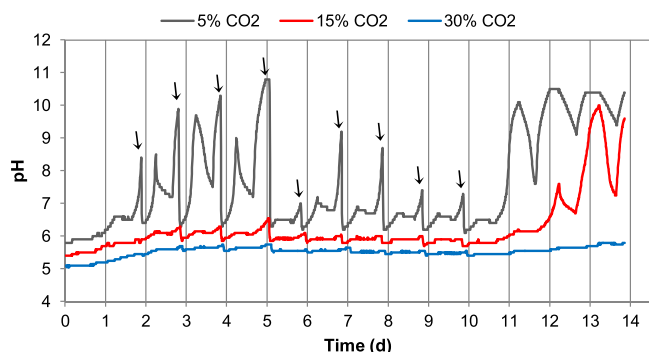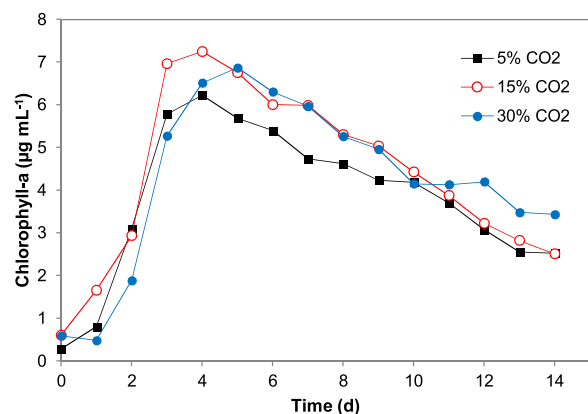

Fig. 5. Chlorophyll-a profiles of *P. kessleri* cultivations under 5, 15 and 30% CO_2.

in *P. kessleri*, very similar to the one obtained in our study under 15% CO_2 (20.8%). In our study, increasing CO_2 concentration did not seem to produce a positive effect on lipid accumulation, as lipid content under 5% CO_2 was approximately 30% higher than under 30% CO_2, although differences were not statistically significant ($p > 0.05$).

The FA composition analysis considered the five major FA present in all evaluated samples (Table 1). For each cultivation condition, the values reported consisted on the percentages of the mean value of the chromatographic peak area for each FA in relation to the sum of chromatographic peak areas of all detected FA. It is also provided the percentage values of saturated fatty acids (SFA), mono-unsaturated fatty acids (MUFA) and poly-unsaturated fatty acids (PUFA) in relation to the total amount of FA detected.

The FA composition of *P. kessleri* presented palmitic acid (16:0), oleic acid (18:1) and linoleic acid (18:2) as the major fatty acids in all the cultivations, although their relative percentages were different depending on the CO_2 concentration. For instance, palmitic acid yields were higher under 30% CO_2 (around 60%) compared to the other conditions (around 30%). In contrast, the amounts of PUFA were higher under 5% CO_2 (around 50%) and decreased to 28.0% and 15.4% under 15 and 30% CO_2, respectively. Another significant difference was on oleic acid production, which increased from almost 14 to 30%, under 5 and 15% CO_2, and decreased to 11% under 30% CO_2. The increase in oleic acid production has been previously reported as an indication of high cell density and accumulation of lipids, normally promoted because of nutrient limitations (van der Ha et al., 2012).

3.3. The impact of CO_2 on carotenoid production

We observed that *P. kessleri* produced extracellular carotenoid-like pigments with colors ranging from yellow to red and varying intensities depending on the CO_2 concentration in the cultivations. Table 2 shows pictures of the algal suspensions (before centrifugation) and the cell-free centrifuged growth media at the end of the cultivations. We hypothesized that the onset for the production of this metabolite is triggered by the stress caused by the lack of CO_2 available, because the reddish color was less intense on cultivations under 30% CO_2, where the interruption on atmosphere renovation most likely did not interfere on the average CO_2 concentration inside the reactor.
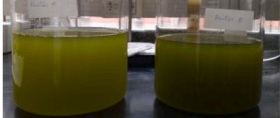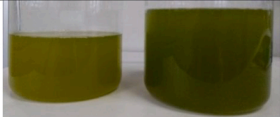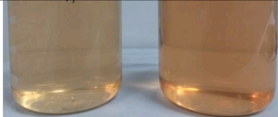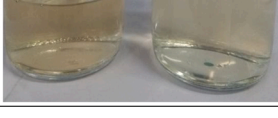
Fig. 6 presents the mean values of total carotenoid concentrations obtained by spectrophotometric measures at 450 nm. According to this methodology, carotenoid production was observed in all cultivations, with concentrations of approximately 0.030 ± 0.005, 0.026 ± 0.006 and 0.011 ± 0.002 μg mL^{-1} under 5, 15 and 30% CO_2, respectively. Total carotenoid content was approximately 16% higher under 5% CO_2 when compared to 15% CO_2, although this difference was not statistically significant ($p > 0.05$). However, the total carotenoid content under 15%

Fig. 4. pH profiles of *P. kessleri* cultivations under 5, 15 and 30% CO_2.

Table 1

Content of major fatty acids and amounts of SFA, MUFA and PUFA in *P. kessleri* cultivated under 5, 15 and 30% CO_2.

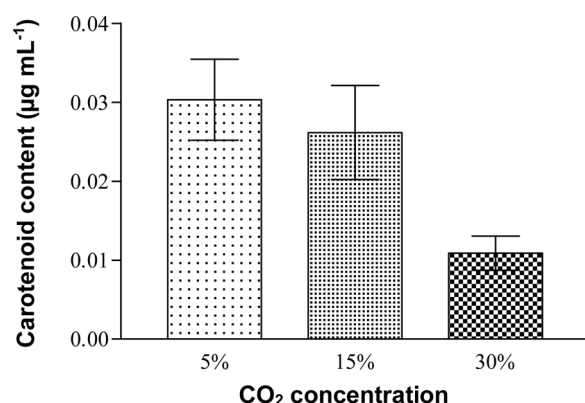| Fatty acid content (%, relative percentage)								
CO_2 concentration (%)	16:0	18:0	18:1	18:2	18:3	SFA	MUFA	PUFA
5	26.0 ± 1.4	8.7 ± 1.2	13.9 ± 6.7	31.0 ± 1.1	20.4 ± 5.8	34.7 ± 2.6	13.9 ± 6.7	51.4 ± 6.9
15	30.3 ± 1.9	9.0 ± 0.2	30.3 ± 0.1	28.0 ± 1.8	ND	39.3 ± 2.1	30.3 ± 0.1	28.0 ± 1.8
30	61.9 ± 11.2	3.5 ± 0.5	11.5 ± 1.8	15.4 ± 5.0	ND	65.4 ± 11.7	11.5 ± 1.8	15.4 ± 5.0

ND – not detected.

Table 2

Final biomass after *P. kessleri* cultivations under different CO_2 concentrations. The algal suspensions before centrifugation are on the left side and the cell-free media are on the right side.

Fig. 6. Total carotenoid concentrations on cell-free media after *P. kessleri* cultivations under CO_2 concentrations of 5, 15 and 30%.

CO_2 was almost 140% higher when compared to 30% CO_2, and this difference was statistically significant ($p < 0.01$).

Although *P. kessleri* is known to produce exopolysaccharides, polysaccharides that are released to the extracellular environment (Raposo et al., 2013), to our knowledge there is no report on extracellular production of carotenoids by this species. Intracellular astaxanthin and lutein productivities from *P. kessleri* obtained by Minhas et al. (2016) were 0.07 and 0.04 mg $L^{-1}d^{-1}$, respectively, and the lutein content was 0.28 mg g^{-1} (dw). These values are higher than the highest concentration of total carotenoids obtained in our study (0.03 mg L^{-1}).

3.4. Carotenoid characterization

The pigment methanolic extracts from *P. kessleri* cultivation under CO_2 conditions of 5, 15 and 30% presented antioxidant activity using the ABTS method (Re et al., 1999), and the same chromatographic profiles in HPLC. They were analysed by HPLC with PDA detector to separate and verify different UV–vis spectra of the fractions.

Two fractions were identified as carotenoid-like because they presented λ_{max} of 405 and 427 nm, the yellow pigment (Fig. 7a), and 455, 485, 524 nm, the red one (Fig. 7b). Adjacent absorbance peaks on these regions of the visible light spectrum are characteristic of carotenoids and indicate multiple chromophore groups (Rodriguez-Amaya, 2001). Both carotenoid fractions were collected in the semi-preparative HPLC for LC—MS/MS analysis.
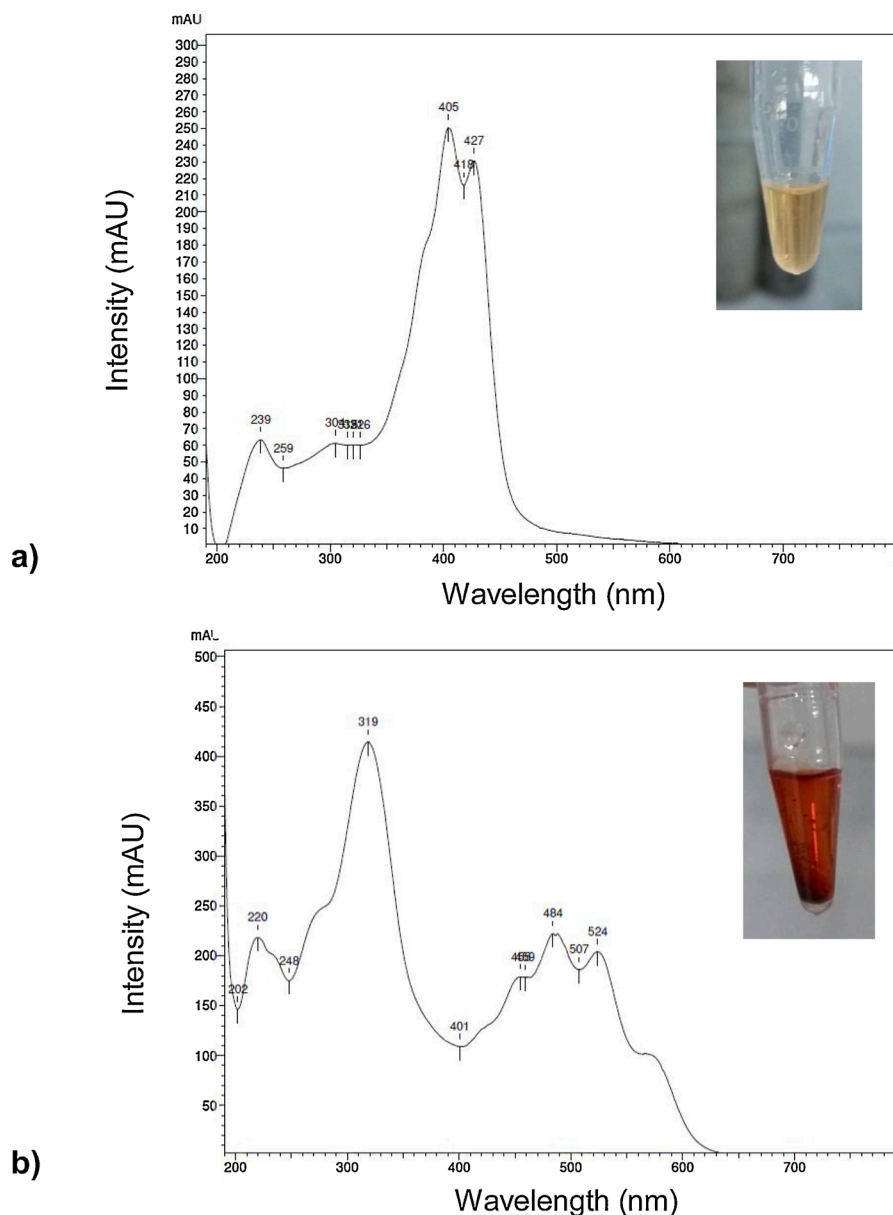
Fig. 7. UV–vis spectra of carotenoid-like fractions obtained after HPLC separation of the pigment methanolic extracts: a) yellow fraction and b) red fraction.

The ESI mass spectrum of the yellow pigment in positive ion mode presented a protonated molecule at m/z 299 ([M+H]$^+$), and its MS/MS fragmentation presented one product ion at m/z 258. With these data its interpretation was not conclusive. On the other hand, the ESI mass spectrum of the red pigment (Fig. 8a) presented two protonated molecules at m/z 285 ([M+H]$^+$) and m/z 569 ([M+H]$^+$), the latter corresponding to the molecular formula $C_{40}H_{56}O_2$ (568.88 g mol^{-1}). A careful analysis of the metabolites in the xanthophyll metabolism of microalgae using Kegg's platform (https://www.genome.jp/kegg/) provided two possible isomers with this molecular formula: zeaxanthin and lutein. However, the protonated molecule at m/z 569 cannot be assigned to one of these isomers, or other unknown isomer, without an elucidative interpretation of the MS/MS spectrum (Fig. 8b), which the product ions are described in Table 3.

In ESI positive mode, carotenoids can produce both molecular ions $M^{\bullet+}$ or protonated molecules [M+H]$^+$, which makes their structural elucidation very complex (Guaratini et al., 2005). Different product ions are present in the MS/MS analysis of carotenoids, which have been proposed as a result of cleavages in the polyene chain of carotenoids,

followed by hydrogen transfer (Neto et al., 2016). The losses of 92 mass units (mu), corresponding to toluene, 106 mu, corresponding to xylene, and 18 mu, corresponding to hydroxyl end groups, are well reported in carotenoids (Atienza et al., 2007; Guaratini et al., 2005).

In Table 3, the product ions in bold are the most abundant, and the others in the second row are less abundant but not less relevant. Among the abundant ions, none of them resulted from the characteristic losses of 18, 92 or 106 mu. Protonated molecules [M+H]$^+$ do not form toluene and xylene fragments using ESI with ion trap (IT) (Weesepoel et al., 2013), at least not with high intensity. However, the product ions in m/z 551 [M+H-18]$^+$, 533 [M+H-18-18]$^+$, 477 [M+H-92]$^+$, and 445 [M+H-18-106]$^+$ were found in much less intensity.

Although the red pigment produced by *P. kessleri*, in this work, is undoubtedly a carotenoid and represent a potential source of high value bioproducts, its structural elucidation was not achieved by the combination of techniques used, remaining as future perspectives.
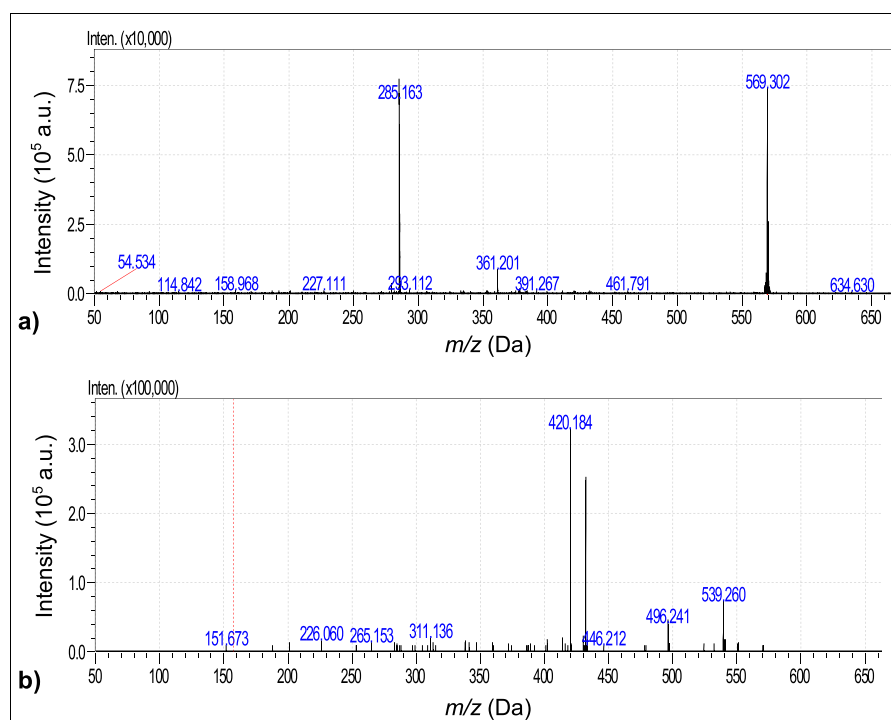
Fig. 8. LC–MS data of the red carotenoid-like pigment produced by *P. kessleri* (a) and MS/MS fragmentation of the protonated molecule at *m/z* 569 (b).

Table 3
MS/MS product ions and λ_{max} (nm) of the red carotenoid-like pigment fraction.

Carotenoid	λ_{max} (nm)	$[M + H]^+$ (*m/z*)	MS/MS product ions (*m/z*)
Red pigment	320, 455, 485, 524	569.3	**539.3; 496.2; 432.2; 420.2** 551 [M+H-18]$^+$; 533 [M+H-18-18]$^+$; 477 [M+H-92]$^+$; 445 [M+H-18-106]$^+$;

4. Discussion

The lipid composition of microalgae may vary according to the culture conditions. The lack of nutrients and high cell density may interfere on the lipid composition; unsaturated FA are normally consumed as energy source and SFA are accumulated (Renaud et al., 2002; Andrade et al., 2015). Indeed, the increase on SFA and MUFA during nutrient starvation has been well reported (Lim et al., 2012), and this can probably explain the increase on SFA with increasing amounts of CO_2 in our cultivations.

Oils with proper characteristics for biodiesel production have been reported, showing highly balanced composition of SFA, MUFA and PUFA (Nascimento et al., 2015). Biodiesel feedstock with a high degree of saturation is more resistant to oxidation and more stable in presence of light, oxygen, high temperatures, and metals (Mutanda et al., 2011). Nevertheless, while this approach may prove useful for biodiesel production, the reduction in PUFA on microalgae FA composition is an issue for high value ω-3 production for commercialization (Lim et al., 2012) (Borowitzka, 2013).

In this respect, the present report suggests that the CO_2 levels on the cultivations impacted on the potential biotechnological application of the biomass. High CO_2 concentrations of 15 and 30% elevated SFA and MUFA in *P. kessleri*, making more suitable for biodiesel production, while drastically decreased ω-3 (18:3). On the other hand, 5% CO_2 may be a strategy for the production of PUFA for a high value market. Thus,

for the use of CO_2 sources other than atmospheric air, the CO_2 concentration should be evaluated according to the desired application.

To our knowledge, the only report on microalgae extracellular carotenoid production was the one by *Botryococcus braunii,* and the main component produced was the ketocarotenoid equinenone (Cheng et al., 2019). This species is known to produce extracellular hydrocarbons as sources of biofuels and polysaccharides. It is also known to produce intracellular carotenoids, such as neoxanthin, loroxanthin, violaxanthin, lutein, α-carotene and β-carotene (Cheng et al., 2019).

One of the challenges of natural carotenoid production in large scale is the cost associated with processing. Carotenoid pigment production from microalgae involves harvesting, extraction and downstream processing, which may be challenging. For instance, cells with very small surface area to volume ratio coupled with a multi-layered cell wall can make it extremely recalcitrant to disruption and may require cost demanding extraction methods, which will impact on the final price of the product (Ambati et al., 2019; Novoveska et al., 2019). In addition, most of the extraction methods require dry biomass, which is also energy and cost demanding. In this respect, extracellular pigments represent a potential alternative to overcome these challenges and to develop more sustainable downstream methods.

5. Conclusions

P. kessleri isolated from mangrove sites and selected under 30% CO_2 atmosphere was proved as a high CO_2-tolerant microalga capable of producing an extracellular red carotenoid-like pigment. This work evaluated the growth kinetics, biomass production, fatty acid profile and total carotenoid yields of *P. kessleri* cultivated in photobioreactors under different CO_2 concentrations (5, 15 and 30%), providing parameters to identify potential biotechnological applications of the produced biomass. The kinetics for all tested conditions were similar, although 30% CO_2 required an adaptation phase. Cell dry weight concentrations and CO_2 fixation rates were higher under 15% CO_2, and this corroborates with higher amounts of oleic acid under this condition, which is an indication of high cell density. In contrast, total lipids, PUFA and total carotenoids were higher under 5% CO_2 compared to the other

conditions. The extracellular red pigment is soluble in methanol, presented antioxidant activity and provided UV–vis absorbance characteristic of molecules with multiple chromophore groups. MS analysis of the purified fraction pointed to a compound with molecular weight of 568 g mol^{-1}, which could not be assigned to a specific carotenoid, although its MS/MS fragmentation confirmed the presence of product ions well reported in carotenoids. To our knowledge, this is the first report on extracellular carotenoid production by *P. kessleri*, which is particularly advantageous considering the extraction methods of intracellular carotenoids from microalgae.

Declaration of Competing Interest

The authors declare that they have no known competing financial interests or personal relationships that could have appeared to influence the work reported in this paper.

CRediT authorship contribution statement

Priscila da Costa Carvalho de Jesus: Conceptualization, Investigation, Methodology, Formal analysis, Writing - original draft, Project administration, Funding acquisition. **Maria Anita Mendes:** Methodology, Writing - review & editing. **Elen Aquino Perpétuo:** Project administration, Writing - review & editing. **Thiago Olitta Basso:** Validation, Writing - review & editing, Supervision. **Claudio Augusto Oller do Nascimento:** Conceptualization, Validation, Formal analysis, Writing - review & editing, Supervision, Funding acquisition.

Acknowledgments

References

Ambati, R.R., Gogisetty, D., Aswathanarayana, R.G., Ravi, S., Bikkina, P.N., Lei, B., Su, Y. P., 2019. Industrial potential of carotenoid pigments from microalgae: current trends and future prospects. Crit. Rev. Food Sci. Nutr. 59, 1880–1902.

Andersen, R.A., Berges, J.A., Harrison, P.J., Watanabe, M.M., 2004. Appendix a - Recipes for Freshwater and Seawater Media. Academic Press.

Andrade, L.M., Mendes, M.A., Kowalski, P., Nascimento, C.A.O., 2015. Comparative study of different matrix/solvent systems for the analysis of crude lyophilized microalgal preparations using matrix-assisted laser desorption/ionization time-of-flight mass spectrometry. Rapid Commun. Mass Spectrom. 29, 295–303.

Atienza, S.G., Ballesteros, J., Martin, A., Hornero-Mendez, D., 2007. Genetic variability of carotenoid concentration and degree of esterification among tritordeum (xTritordeum Ascherson et Graebner) and durum wheat accessions. J. Agric. Food Chem. 55, 4244–4251.

Balcombe, P., Anderson, K., Speirs, J., Brandon, N., Hawkes, A., 2015. Methane and CO2 Emissions From the Natural Gas Supply Chain - an Evidence Assessment.

Borowitzka, M.A., 2013. High-value products from microalgae-their development and commercialisation. J. Appl. Phycol. 25, 743–756.

Breuer, G., Evers, W.A.C., De Vree, J.H., Kleingris, D.M.M., Martens, D.E., Wijffels, R.H., Lamers, P.P., 2013. Analysis of fatty acid content and composition in microalgae. Jove-J. Visual. Exp.

Britton, G. (Ed.), 1985. General Carotenoids Methods. Academic Press.

Cezare-Gomes, E.A., Mejia-Da-Silva, L.D., Perez-Mora, L.S., Matsudo, M.C., Ferreira-Camargo, L.S., Singh, A.K., De Carvalho, J.C.M., 2019. Potential of microalgae carotenoids for industrial application. Appl. Biochem. Biotechnol. 188, 602–634.

Chekanov, K., Schastnaya, E., Solovchenko, A., Lobakova, E., 2017. Effects of CO2 enrichment on primary photochemistry, growth and astaxanthin accumulation in the chlorophyte Haematococcus pluvialis. J. Photochem. Photobiol. B-Biol. 171, 58–66.

Cheng, P.F., Okada, S., Zhou, C.X., Chen, P., Huo, S.H., Li, K., Addy, M., Yan, X.J., Ruan, R.R., 2019. High-value chemicals from Botryococcus braunii and their current applications - a review. Bioresour. Technol. 291.

Chisti, Y., 2007. Biodiesel from microalgae. Biotechnol. Adv. 25, 294–306.

Da Silveira, C.A., 2015. Modelagem e simulação de reator de cultivo de microalgas tipo "open pond". Ph.D, Universidade de São Paulo.

De Morais, M.G., Costa, J.A.V., 2007. Isolation and selection of microalgae from coal fired thermoelectric power plant for biofixation of carbon dioxide. Energy Convers. Manage. 48, 2169–2173.

Fung, C.J., 2002. The effect of headspace pressure on the performance of a fluidised-bed bioreactor. J. Chem. Technol. Biotechnol. 77, 1186–1190.

Gracioso, L.H., Bellan, A., Karolski, B., Cardoso, L.O.B., Perpetuo, E.A., Nascimento, C.A. O., Giudici, R., Pizzocchero, V., Basaglia, M., Morosinotto, T., 2020. Light excess stimulates Poly-beta-hydroxybutyrate yield in a mangrove-isolated strain of Synechocystis sp. Bioresour. Technol. https://doi.org/10.1016/j.biortech.2020.124379.

Guaratini, T., Vessecchi, R., Pinto, E., Colepicolo, P., Lopes, N.P., 2005. Balance of xanthophylls molecular and protonated molecular ions in electrospray ionization. J. Mass Spectrom. 40, 963–968.

Kassim, M.A., Meng, T.K., 2017. Carbon dioxide (CO2) biofixation by microalgae and its potential for biorefinery and biofuel production. Sci. Total Environ. 584, 1121–1129.

Klinthong, W., Yang, Y.H., Huang, C.H., Tan, C.S., 2015. A review: microalgae and their applications in CO2 capture and renewable energy. Aerosol Air Qual. Res. 15, 712–742.

Krinsky, N.I., Landrum, J.T., Bone, R.A., 2003. Biologic mechanisms of the protective role of lutein and zeaxanthin in the eye. Annu. Rev. Nutr. 23, 171–201.

Li, X.L., Pribyl, P., Bisova, K., Kawano, S., Cepak, V., Zachleder, V., Cizkova, M., Branyikova, I., Vitova, M., 2013. The microalga Parachlorella kessleri–A novel highly efficient lipid producer. Biotechnol. Bioeng. 110, 97–107.

Li, D.J., Wang, L., Zhao, Q.Y., Wei, W., Sun, Y.H., 2015. Improving high carbon dioxide tolerance and carbon dioxide fixation capability of Chlorella sp by adaptive laboratory evolution. Bioresour. Technol. 185, 269–275.

Lim, D.K., Garg, S., Timmins, M., Zhang, E.S., Thomas-Hall, S.R., Schuhmann, H., Li, Y., Schenk, P.M., 2012. Isolation and evaluation of oil-producing microalgae from subtropical coastal and brackish waters. PLoS One 7, e40751.

Masood, A., Stark, K.D., Salem, N., 2005. A simplified and efficient method for the analysis of fatty acid methyl esters suitable for large clinical studies. J. Lipid Res. 46, 2299–2305.

Minhas, A.K., Hodgson, P., Barrow, C.J., Sashidhar, B., Adholeya, A., 2016. The isolation and identification of new microalgal strains producing oil and carotenoid simultaneously with biofuel potential. Bioresour. Technol. 211, 556–565.

Mutanda, T., Ramesh, D., Karthikeyan, S., Kumari, S., Anandraj, A., Bux, F., 2011. Bioprospecting for hyper-lipid producing microalgal strains for sustainable biofuel production. Bioresour. Technol. 102, 57–70.

Nascimento, I.A., Cabanelas, I.T.D., Dos Santos, J.N., Nascimento, M.A., Sousa, L., Sansone, G., 2015. Biodiesel yields and fuel quality as criteria for algal-feedstock selection: effects of CO2-supplementation and nutrient levels in cultures. Algal Res.-Biomass Biofuels Bioprod. 8, 53–60.

Neto, F.C., Guaratini, T., Costa-Lotufo, L., Colepicolo, P., Gates, P.J., Lopes, N.P., 2016. Re-investigation of the fragmentation of protonated carotenoids by electrospray ionization and nanospray tandem mass spectrometry. Rapid Commun. Mass Spectrom. 30, 1540–1548.

Novoveska, L., Ross, M.E., Stanley, M.S., Pradelles, R., Wasiolek, V., Sassi, J.F., 2019. Microalgal Carotenoids: A Review of Production, Current Markets, Regulations, and Future Direction. Mar. Drugs 17.

Pruvost, J., Van Vooren, G., Le Gouic, B., Couzinet-Mossion, A., Legrand, J., 2011. Systematic investigation of biomass and lipid productivity by microalgae in photobioreactors for biodiesel application. Bioresour. Technol. 102, 150–158.

Raposo, M.F.D., De Morais, R., De Morais, A., 2013. Bioactivity and Applications of Sulphated Polysaccharides from Marine Microalgae. Mar. Drugs 11, 233–252.

Re, R., Pellegrini, N., Proteggente, A., Pannala, A., Yang, M., Rice-Evans, C., 1999. Antioxidant activity applying an improved ABTS radical cation decolorization assay. Free Radic. Biol. Med. 26, 1231–1237.

Ritchie, R.J., 2006. Consistent sets of spectrophotometric chlorophyll equations for acetone, methanol and ethanol solvents. Photosyn. Res. 89, 27–41.

Rodriguez-Amaya, D.B., 2001. A Guide to Carotenoid Analysis in Foods.

Salih, F.M., 2011. Microalgae tolerance to high concentrations of carbon dioxide: a review. J. Environ. Prot. 02, 648–654.

Singh, S.P., Singh, P., 2014. Effect of CO2 concentration on algal growth: A review. Renewable Sustainable Energy Rev. 38, 172–179.

Sun, Z.L., Chen, Y.F., Du, J.C., 2016. Elevated CO2 improves lipid accumulation by increasing carbon metabolism in Chlorella sorokiniana. Plant Biotechnol. J. 14, 557–566.

Van Der Ha, D., Nachtergaele, L., Kerckhof, F.M., Rameiyanti, D., Bossier, P., Verstraete, W., Boon, N., 2012. Conversion of Biogas to Bioproducts by Algae and Methane Oxidizing Bacteria. Environ. Sci. Technol. 46, 13425–13431.

Weesepoel, Y., Vincken, J.P., Pop, R.M., Liu, K., Gruppen, H., 2013. Sodiation as a tool for enhancing the diagnostic value of MALDI-TOF/TOF-MS spectra of complex astaxanthin ester mixtures from Haematococcus pluvialis. J. Mass Spectrom. 48, 862–874.

Wilson, M.H., Mohler, D.T., Groppo, J.G., Grubbs, T., Kesner, S., Frazar, E.M., Shea, A., Crofcheck, C., Crocker, M., 2016. Capture and recycle of industrial CO2 emissions using microalgae. Appl. Petrochem. Res. 6, 279–293.

Yadav, G., Karemore, A., Dash, S.K., Sen, R., 2015. Performance evaluation of a green process for microalgal CO2 sequestration in closed photobioreactor using flue gas generated in-situ. Bioresour. Technol. 191, 399–406.

Yan, C., Munoz, R., Zhu, L.D., Wang, Y.X., 2016. The effects of various LED (light emitting diode) lighting strategies on simultaneous biogas upgrading and biogas slurry nutrient reduction by using of microalgae Chlorella sp. Energy 106, 554–561.

Zhu, C.J., Lee, Y.K., 1997. Determination of biomass dry weight of marine microalgae. J. Appl. Phycol. 9, 189–194.